View metadata, citation and similar papers at core.ac.uk
brought to you by CORE
provided by Elsevier - Publisher Connector

Soils and Foundations 2013;53(4):487–497

The Japanese Geotechnical Society

Soils and Foundations

www.sciencedirect.com
journal homepage: www.elsevier.com/locate/sandf

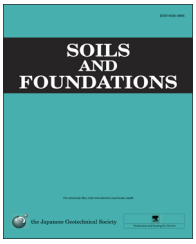

Design method for stabilization of earth slopes with micropiles

Shu-Wei Sun[a,*], Ben-Zhen Zhu[b], Jia-Chen Wang[a]

[a]*Faculty of Resources and Safety Engineering, China University of Mining and Technology (Beijing), Beijing 100083, China*
[b]*Northwest Research Institute Co., Ltd. of C.R.E.C., Lanzhou 730000, China*

Received 17 July 2012; received in revised form 18 March 2013; accepted 6 April 2013
Available online 29 July 2013

Abstract

As one of the measures for slope fast reinforcement, micropiles are always designed as a group. In this paper, an analytic model for the ultimate resistance of micropile is proposed, based on a beam–column equation and an existing *p–y* curve method. As such, an iterative process to find the bending moment and shear capacity of the micropile section has been developed. The formulation for calculating the inner force and deflection of the micropile using the finite difference method is derived. Special attention is given to determine the spacing of micropiles with the aim of achieving the ultimate shear capacity of the micropile group. Thus, a new design method for micropiles for earth slope stabilization is proposed that includes details about choosing a location for the micropiles within the existing slope, selecting micropile cross section, estimating the length of the micropile, evaluating the shear capacity of the micropiles group, calculating the spacing required to provide force to stabilize the slope and the design of the concrete cap beam. The application of the method to an embankment landslide in Qinghai province, China, is described, and monitoring data indicated that slope movement had effectively ceased as a result of the slope stabilization measure, which verified the effectiveness of the design method.
© 2013 The Japanese Geotechnical Society. Production and hosting by Elsevier B.V. All rights reserved.

Keywords: Earth slope stabilization; Micropiles group; Design method; Finite difference method; *p–y* Curve

1. Introduction

Slope failures often result in extensive property damage and sometimes loss life. Improving the stability of both natural and manmade slopes continues to be a fundamental problem in geotechnical engineering.

One method that has been used to improve the stability of slopes has been via the installation of micropiles. Micropiles are defined as small-diameter (typically less than 300 mm), drilled and grouted replacement piles that are typically reinforced (Bruce and Juran, 1997). A micropile is constructed by drilling a borehole, placing reinforcement, and grouting the hole. Micropile technology has evolved continuously since its introduction by Fernando Lizzi in the 1950s. Over the past 60 years, advances in drilling equipment and techniques have extended the applicability of micropiles to infrastructure repair and seismic retrofit projects (Tsukada et al., 2006; Pinyol and Alonso, 2012). Compared to conventional anti-sliding piles, micropiles construction is relatively simple, fast, environmental-friendly and economic. Besides, micropiles can be readily installed in areas with limited equipment access, such as for landslides located in hilly, steep, or mountainous areas. The successful use of this method in slope stabilization has been described by several investigators (for example, Lizzi, 1978; Cantoni et al., 1989; Pearlman et al., 1992; Juran et al., 1996; Loehr et al., 2000; Sun et al., 2009).

Despite these applications, the methods used for the design of the stabilization micropiles vary widely. Lizzi (1978) suggests that micropiles can be used as the reticulated network

*Corresponding author. Tel.: +86 10 6233 9153; fax: +86 10 6233 9052.
E-mail address: sunshuwei@cumtb.edu.cn (S.-W. Sun).
Peer review under responsibility of The Japanese Geotechnical Society.

Production and hosting by Elsevier

0038-0806 © 2013 The Japanese Geotechnical Society. Production and hosting by Elsevier B.V. All rights reserved.
http://dx.doi.org/10.1016/j.sandf.2013.06.002

Nomenclature

p	soil response
y	micropile deflection
dx	length of micropile element
Δ	deformation at any distance from the neutral axis of the element
$d\theta$	relative rotation of the sides of the element
ρ	radius of curvature of the elastic element
η	distance from the neutral axis
ε_x	unit strain along the length of the micropile
ϕ	curvature of the elastic element
EI	flexural rigidity
E	modulus of elasticity
I	moment of inertia
M_{ult}	ultimate moment capacity of micropile
P_x	vertical compressive force
M	bending moment
dM	increment of bending moment
M	bending moment of micropile
Q	shearing force of micropile
N	axial force of micropile
E_s	elastic foundation coefficient
W	landslide thrust
R_m	flexural rigidity at point m
$\overline{\varphi}_m$	angle of rotation
M_{max}	maximum bending moment along the micropile
M_0	trial bending moment at boundary
Q_0	trial shear force at boundary
Q_{ult}	shear capacity of a veritical micropile
$\overline{Q}_{ult}$	shear capacity of an inclined micropile
N_{ult}	maximum axial resistance of micropile
ψ	inclined angle of micropile
α_1	grout-to-ground ultimate bond strength above the ciritcal slip surface
α_2	grout-to-ground ultimate bond strength below the critical slip surface
L_1	length of micropile above the critical slip surface
L_2	length of micropile below the critical slip surface
d	diameter of a micropile
D_1	center-to-center distance between micropiles in a row
$D_{1,\ max}$	maximum center-to-center distance between micropiles in a row
D_2	opening between micropiles in a row
$\overline{D_1}$	center-to-center distance between in-line micropiles
FS	the required factor of safety
F_R	force required to increase the factor of safety
F_1	shear capacity of battered upslope micropiles
F_2	shear capacity of vertical micropiles
F_3	shear capacity of battered downslope micropiles
F_A	combined capacity of micropiles group
c	cohesion of the soil
φ	angle of internal friction of soil
q	lateral force acting on the micropile due to soil movement
F_q	q intergrated over the length of the micropile above the critical slip surface
γ'	effective unit weight of the soil
c_u	undrained strength of the soil
ε_{50}	strain corresponding to one-half of the maximum principal stress difference

system, which creates a stable reinforced soil as "gravity-retaining wall", and the reinforced soil gravity mass supplies the essential lateral loads due to the movement of the unstable slope. Hence, Lizzi (1982) proposed a design method for micropiles groups based on assumption that it is a highly redundant system in which no tension is applied to any of the micropiles. This system is subjected to compression and shear and the micropiles provide confinement to the in-situ soil, thereby improving its deformation modulus and increasing its shear resistance. The behavior of this system depends to a great extent on the "knot effect" (Lizzi, 1978; Plumelle, 1984) concept and the reinforced concrete analogy. In actual fact, however, the mechanism of the knot effect is very complex and many of the factors which influence the final behavior of the structure cannot be reasonably assessed, so the design method has limited applicability. Palmerton (1984) and Pearlman and Wolosick (1992) suggest that micropiles can be designed to transfer axial and lateral loads through soft or weak soils to more competent strata. These micropiles are generally used to resist the applied loads directly. This design concept relies mainly on substituting conventional large-diameter pile types with closely spaced, small-diameter, high-strength piles to arrest sliding body. However, the comparative tests between micropiles and conventional anti-sliding piles conducted by Sun et al. (2009) showed that micropiles were totally different from anti-sliding pile with regard to the loading mechanism. With larger flexural rigidity, conventional piles suffered inclination deformation result from compression fracture of soil behind pile. With smaller flexural rigidity, micropiles suffered flexible deformation, which also made the plastic zone of soil among micropiles cross and overlap, so the larger lateral displacement occurred at the sliding surface and on the top of the micropile. Therefore, the solution for conventional piles cannot be easily adapted to micropiles. Loehr et al. (2000) proposed a simplified method for predicting the limit resistance of recycled plastic reinforcement for application to stabilization of minor slopes. In their method, which is based on elastic analyses, two general failure mechanisms are considered to determine the distribution of limit lateral resistance along the reinforcing members: failure of soil around or between reinforcing members and structural failure of the reinforcing member due to mobilized forces from the surrounding soil. Reese et al. (1992) also described a procedure for the design of slopes stabilized with micropiles.

The method calculates the resistance provided by micropiles assuming that the limit state is the failure of the micropile in bending and subsequently checking the potential for soil failure leading to flow of the soil between micropiles. An important assumption included in the method is that the axial forces that develop in the micropiles only affect the stability by increasing the lateral resistance provided by the micropiles. The axial components normal to the sliding surface are not included explicitly in the stability analysis, so effects such as decreasing the normal force on the base of a slice are ignored. In general, the design methods for stabilization of slopes with micropiles groups are not mature, and some of the designs have generally been very conservative out of necessity.

The purpose of this paper is to set out a more reliable design method for the micropiles groups as a measure against landslide. First, an analytic model for ultimate resistance of micropiles is set up, using a beam–column equation and an existing p–y curve method, to find the bending moment and shear capacity of the micropile. Then, a step-by-step design procedure for micropiles is introduced, including how to choose the location for the micropile group within an existing slope, how to select the micropile cross section and estimate the length of the micropile, how to evaluate the shear capacity of the micropile group, and how to calculate the required spacing and design the concrete cap beam. Finally, the application of the method to an embankment slope hazard problem in Qinghai province, China is described.

2. Evaluation of bending moment capacity of micropile

Because they are slender reinforcements, the stiffness and lateral resistance of individual micropiles is generally small. Therefore, when micropiles are used to stabilize earth slopes, the interaction between the micropile and soil makes them susceptible to bending failure. The shear resistance of a micropile corresponds to the maximum shear force that can be applied to the micropile that results in a maximum bending moment within the micropile just equal to the ultimate bending moment of the micropile. Hence, the ultimate bending moment of the single micropile needs to be obtained to evaluate the shear resistance of a single micropile.

An element from a micropile with an unloaded shape of *abcd* is shown by the dashed lines in Fig. 1. The beam is subjected to pure bending and element changes in shape as shown by the solid lines. The length of element is given by dx and the deformation at any distance from the neutral axis is signified by Δ. The relative rotation of the sides of the element is given by the small angle dθ and the radius of curvature of the elastic element is signified by the length ρ. The symbol η is the distance from the neutral axis. The unit strain ε_x along the length of the micropile can be expressed as

$$\varepsilon_x = \frac{\Delta}{\mathrm{d}x} \tag{1}$$

From similar triangles

$$\frac{\rho}{\mathrm{d}x} = \frac{\eta}{\Delta} \tag{2}$$

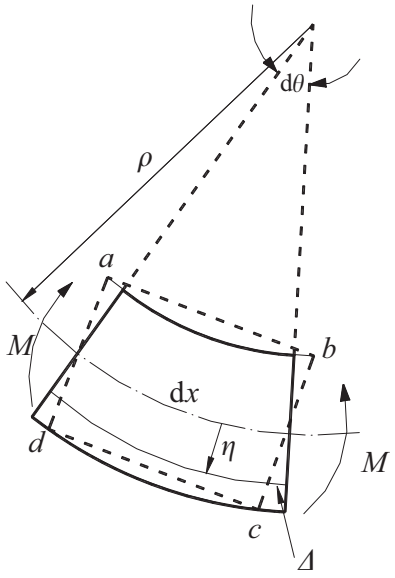

Fig. 1. Deformation shape of an element from a micropile.

It can be seen that dx=ρ dθ and

$$\frac{1}{\rho} = \frac{\mathrm{d}\theta}{\mathrm{d}x} = \phi \tag{3}$$

where ϕ is the curvature.

From Eqs. (1) to (3), the following equation is found:

$$\varepsilon_x = \phi\eta \tag{4}$$

The flexural behavior of the micropile subjected to bending is dependent upon its flexural rigidity, EI, where E is the modulus of elasticity of the material of which it is made and I is the moment of inertia of the cross section about the axis of bending. Because of the nonlinearity in the micropole stress–strain relationships, the value of E varies, and because the concrete in the tensile zone below the neutral axis becomes ineffective due to cracking, the value of I is reduced. Besides, since micropiles are made up of a composite cross section, there is no way to calculate directly the value of E as a whole. The ultimate moment capacity M_{ult} of a micropile can be obtained based on the following procedure:

Step 1: selecting a value of ϕ and estimating the position of the neutral axis. The strain at points along the depth of the micropile can be computed by use of Eq. (4), which in turn will lead to the forces in the concrete and steel. With the magnitude of the forces, both tension and compression, the equilibrium of the section can be checked, taking into account the external compressive loading. If the section is not in equilibrium, a revised position of the neutral axis is selected and iterations proceed until the neutral axis is found.

Step 2: the bending moment is found from the forces in the concrete and steel by taking moments about the centroidal axis of the section.

Step 3: the maximum strain is tabulated and the solution proceeds by incrementing the value of ϕ. The computations continue until the maximum strain selected for failure in the

concrete or in a steel tube is reached or exceeded. Thus, the ultimate moment M_{ult} that can be sustained by the micropile section can be found.

Here, assumptions are made that the stress–strain curves of concrete and steel adopted for the analysis are from (Hognestad, 1951; Rusch, 1960). The ultimate bending moment of a reinforced-concrete section is taken at a maximum strain of concrete of 0.003 and is not affected by the crack spacing. Because of the large amount of deformation of steel when it is stressed to beyond the proportional limit, the ultimate bending moment for steel is considered to occur at a maximum strain of 0.015, which is five times that of concrete.

3. Method of analysis of micropile resistance

The fundamental objective for designing stabilization schemes with micropiles is to determine the resistance that can be provided by individual micropiles as well as the number of micropiles required to increase the stability of a slope to an acceptable level. Given the lateral resistance of individual micropiles, the mechanics of stability analysis for slopes reinforced with structure members is relatively straightforward and well established. Thus, the primary need in designing micropiles stabilization schemes is to determine or estimate the resisting forces provided by each micropiles.

3.1. Evaluation of shear capacity of single vertical micropile

The nonlinear curve relating the soil response and the pile deflection is always termed as a p–y curve, where y is the pile deflection and p is the soil response. Some writers have made use of the theory of elasticity to develop expressions for p as a function of y, but the approach has been of limited use. Soil behavior can be modeled by the theory of elasticity only for very small strains. The common characteristic shape of p–y curves for static and cyclic loading in clay adopted for the analysis are from Matlock (1970) and Reese and Welch (1975), which were obtained from site tests. Thus, an analytic model for evaluating the shear capacity of single vertical micropile can be set up based on the existing p–y curve method and conventional beam–column equation.

For simplicity, the micropile can be assumed to be a bar. A segment bounded by two horizontals a distance of dx apart has been cut from the bar as shown in Fig. 2. The segment has been displaced due to lateral loading and a pair of vertical compressive forces P_x are acting at the center of gravity of the end cross sections of the bar.

The equilibrium of moments (ignoring second-order terms) leads to the equation:

$$\frac{dM}{dx} + P_x \frac{dy}{dx} - Q = 0 \tag{5}$$

where M is the bending moment; dM is the increment of bending moment and Q is the shearing force.

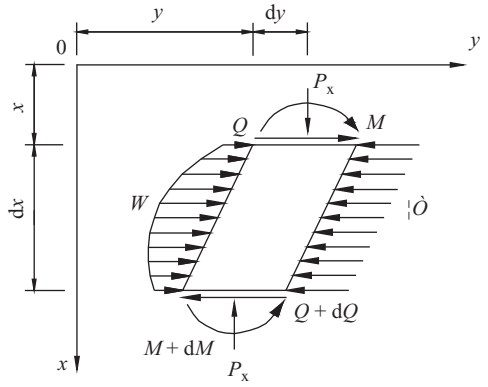

Fig. 2. Analysis of element of a micropile.

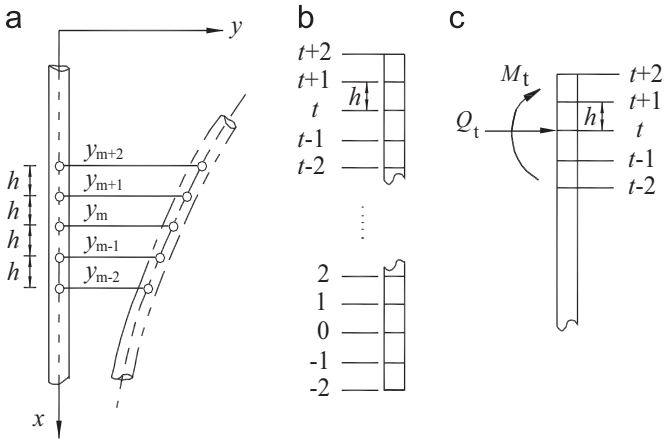

Fig. 3. Deflection and differential points of deflected micropile.

Differentiating Eq. (5) with respect to x, the following equation is obtained:

$$\frac{d^2M}{dx^2} + P_x \frac{d^2y}{dx^2} - \frac{dQ}{dx} = 0 \tag{6}$$

The following identities are noted:

$$\frac{d^2M}{dx^2} = EI\frac{d^4y}{dx^4} \tag{7}$$

$$\frac{dQ}{dx} = -E_s y \tag{8}$$

where E_s is the elastic foundation coefficient.

The term W is added to allow a distributed load to be placed along the micropile as landslide thrust. And the following equation can be obtained:

$$\frac{d^2M}{dx^2} + P_x \frac{d^2y}{dx^2} + E_s y - W = 0 \tag{9}$$

Eq. (9) can be solved readily by using finite-difference techniques. The deflection of the pile by finite deflections is shown in Fig. 3a. The finite difference expressions for the first

two terms of the equation at point m are:

$$\left(\frac{d^2M}{dx^2}\right)_m = \left[y_{m-2}R_{m-1} + y_{m-1}(-2R_m - 2R_{m-1}) + y_m(4R_m + R_{m-1} + R_{m+1}) + y_{m+1}(-2R_m - 2R_{m+1}) + y_{m+2}R_{m+1}\right]\frac{1}{h^4} \quad (10)$$

$$P_x\left(\frac{d^2y}{dx^2}\right)_m = \frac{P_x(y_{m-1} - 2y_m + y_{m+1})}{h^2} \quad (11)$$

where R_m is the flexural rigidity at point (m) and $R_m = E_m I_m$.

Eqs. (10) and (11) are substituted for terms in Eq. (9) and the resulting equation for point m along the pile is

$$y_{m-2}R_{m-1} + y_{m-1}(-2R_{m-1} - 2R_m + P_x h^2) + y_m(R_{m-1} + 4R_m + R_{m+1} - 2P_x h^2 + E_{sm}h^4) + y_{m+1}(-2R_m - 2R_{m+1} + P_x h^2) + y_{m+2}R_{m+1} - W_m h^4 = 0 \quad (12)$$

Using the notation shown in Fig. 3b and c, the boundary conditions at the bottom and top of the micropile are as following, which can be applied to solve the differential equation in difference form.

The bending moment and the shear force at the bottom of the micropile are zero:

$$y_{-1} - 2y_0 + y_1 = 0 \quad (13)$$

$$y_{-2} = y_{-1}\left(2 - \frac{P_x h^2}{R_0}\right) - y_1\left(2 - \frac{P_x h^2}{R_0}\right) + y_2 \quad (14)$$

The lateral load Q_t and the moment M_t at the top of the micropile are known ($m = t$):

$$\frac{R_t}{2h^3}(y_{t-2} - 2y_{t-1} + 2y_{t+1} - y_{t-2}) + \frac{P_x}{2h}(y_{t-1} - y_{t+1}) = Q_t \quad (15)$$

$$\frac{R_t}{h^2}(y_{t-1} - 2y_t + y_{t+1}) = M_t \quad (16)$$

The differential equation can be solved based on the following procedures:

Step 1: Selecting a value of E_{sm} at any point m, Eqs. (13)–(16) are substituted for terms in Eq. (12) and get the value of y_m at point m.
Step 2: Obtain the value of p_m with y_m from the family of p–y curves.
Step 3: Iteration is carried out until the solution converges to approximate values of E_s at all points along the micropile.

After the above process, the angle of rotation, the bending moment and shearing force along the micropile can be obtained from Eqs. (17) to (19).

$$\overline{\varphi}_m = \frac{y_{m-1} - y_{m+1}}{2h} \quad (17)$$

$$M_m = \frac{R_m}{h^2}(y_{m-1} - 2y_m + y_{m+1}) \quad (18)$$

$$Q_m = \frac{R_m}{2h^3}(y_{m-2} - 2y_{m-1} + 2y_{m+1} - y_{m+2}) \quad (19)$$

The maximum shear force that the micropile can carry corresponds to that shear force applied at the elevation of the slip surface, which results in a calculated maximum bending moment in the micropile M_{max}, which is equal to M_{ult}. Fig. 4 shows the analytic model proposed to determine the shear force capacity of a single micropile. Here, the shear force capacity of a single vertical micropile is determined by separately analyzing the portion of the micropile above the potential slip surface and the portion of the micropile below the potential slip surface.

The process to determine the maximum shear capacity requires performing up and down analyses as a set. The shear capacity of a single vertical micropile (Q_{ult}) can be determined based on the following procedures:

Step 1: Selecting the value of Q_0 and M_0 (see Fig. 4) as the trial boundary shear forces and bending moments, which is applied at the slip surface location. Here, the head of the micropile is modeled as free, and the input shear force magnitude and direction applied at the slip surface location is the same for the up and down analyses. Besides, the input bending moment is equal in magnitude and opposite in sign for the up and down analyses.

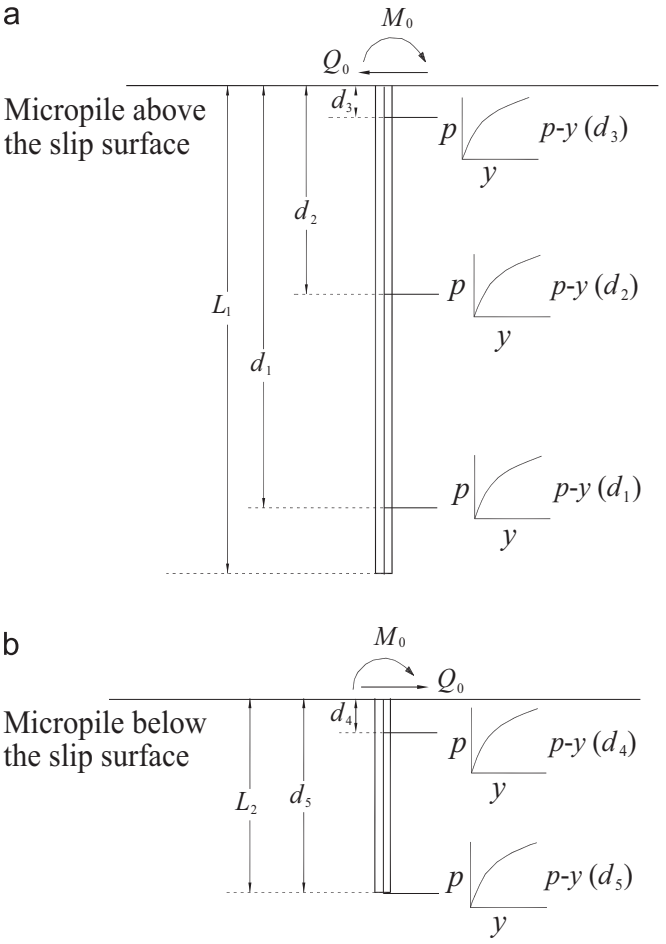

Fig. 4. Analytical model for ultimate resistance of micropile.

Step 2: Run the iterative process of up analysis and down analysis using Eqs. (12) and (17)–(19), respectively. On the basis of deformation compatibility condition, the calculated slope of the micropile head at the slip surface should be the same for the up and down analyses.

Step 3: Comparing the calculated bending moment along the micropile M_{max} to M_{ult}, the process is termined for the case where M_{max}=M_{ult} and the micropile head slope from the up and down analysis is equivalent.

3.2. Evaluation of shear capacity of single inclined micropile

The installed of micropiles in a group with some inclined micropiles has also been advocated. The maximum lateral force ($\overline{Q}_{ult}$) that an inclined single micropile can resist at the location of the critical surface can be evaluated by the limit equilibrium method.

Fig. 5 shows the assumed forces acting on a micropile for the case of a vertical micropile and for an inclined micropile. The inclined angle (ψ) is defined as the angle between the slip surface and the vertical axis of the micropile. Adding the shear and axial forces shown in Fig. 5b in the x direction results in the following:

$$\overline{Q}_{ult} = Q_{ult}\cos\psi + N\sin\psi \tag{20}$$

where N is the axial force of the micropile.

It was noted by Poulos and Davis (1980) that the maximum axial resistance can be assumed to develop in a pile inclined at approximately 30°. This conclusion is employed to micropiles for lack of site test data. Therefore, the maximum lateral force that an inclined single micropile can resist at the location of the critical slip surface can be determined as

(1) For $0^\circ \le \psi \le 10^\circ$, $\overline{Q}_{ult} = Q_{ult}$.
(2) For $\psi \ge 30^\circ$, $\overline{Q}_{ult}$ is determined by Eq. (20); and the N is replaced as the maximum axial resistance (N_{ult}) defined as

$$N_{ult} = \alpha_1 L_1 \pi d \tag{21}$$

where α_1 is the grout-to-ground ultimate bond strength above the critcal slip surface; L_1 (see Fig. 4) is the length of micropile above the critical slip surface; d is the diameter of a micropile.
(3) For $10^\circ < \psi < 30^\circ$, $\overline{Q}_{ult}$ is interploted by (1) and (2).

4. Design methodology of micropiles to increase earth slope stability

The general design approach for micropiles in a group to increase earth slope stability involves six main steps: (1) choosing a location for the micropiles within the existing slope; (2) selecting the micropile cross section; (3) estimating length of micropile; (4) evaluating shear capacity of micropile group; (5) calculating spacing required to provide force to stabilize the slope; and (6) design of concrete cap beam.

4.1. Choosing a location for the micropile group

The lateral location of the piles is often found to be in the vicinity of the midpoint of the slope (Poulos, 1995; Cai and Ugai, 2000). However, the magnitude of force required to increase the factor of safety of the slope (F_R) will vary depending on the location of the micropile group within the slope. It is clear that, in order to be effective, the following factors should be taken into account: (1) micropiles should

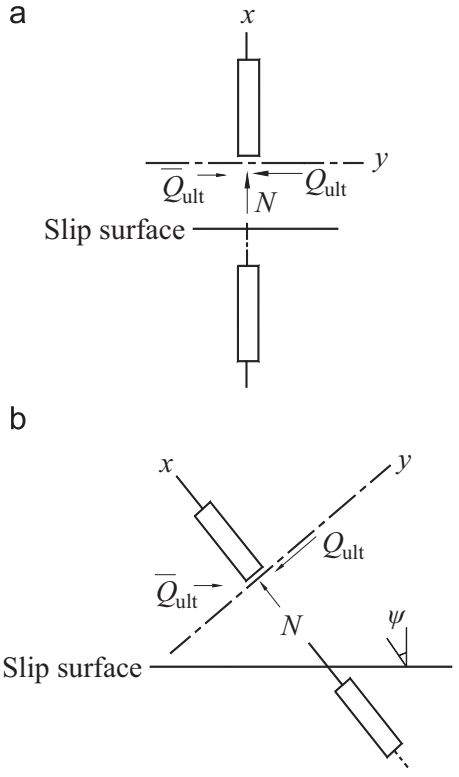

Fig. 5. Forces acting on micropile at slip surface. (a) Vertical micropile and (b) Inclined micropile.

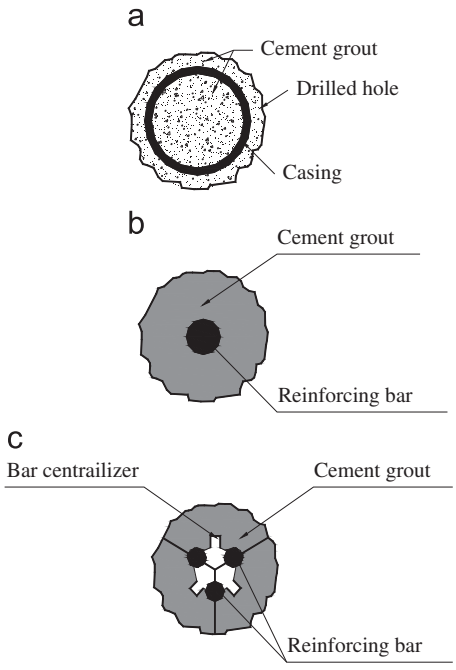

Fig. 6. Types of micropile cross section. (a) Type A, (b) Type B and (c) Type C.

provide the required resistance for the slope to achieve the target factor of safety; and (2) other possible slip surfaces away from the micropiles should be investigated also to check whether a more critical surface existed and had factor of safety values less than the target value. If that was the case, the additional measures should be taken to increase the local slope stability.

4.2. Selecting micropile cross section

Micropile cross sections commonly used in engineering practice are illustrated as shown in Fig. 6. Reinforcement may consist of a single reinforcing bar, a group of reinforcing bars, a steel pipe casing or rolled structural steel. Grout can be sand-cement mortars or neat cement grouts placed under the gravity head or pressures typically ranging from 0.5 to 8 MPa. Grouting is required to be completed within 12 h after boring to restrain the loosening of soil around the bored micropiles according to the Chinese standard GB 50330-2002. In actual fact, the mechanism of loosening is very complex and there are many factors which influence the final behavior in ways that cannot be conveniently assessed. As such, for the sake of simplicity, the loosening effect of soil around the bored pile was not taken into account in the design approach.

4.3. Estimating length of micropile

The length of micropile above the ciritical slip surface, L_1 can be obtained approximately based on the selected micropile location. The side resistance capacity of the micropile below the potential slip surface must be sufficient to resist the axial forces which developed above the potential slip surface. Therefore, the length of micropile below the critical slip surface, L_2, should be selected following the rule:

$$\alpha_2 L_2 \pi d \geq p_{ult} = \alpha_1 L_1 \pi d\, FS \tag{22}$$

where α_2 is the grout-to-ground ultimate bond strength below the critical slip surface, and FS is the required factor of safety.

From Eq. (22), one can obtain

$$L_2 \geq \frac{\alpha_1}{\alpha_2} \cdot L_1\, FS \tag{23}$$

Total length (L) of the micropile can be calculated as

$$L = L_1 + L_2 \tag{24}$$

4.4. Evaluating shear capacity of micropiles

Experimental studies by Holloway et al. (1981) and Brown et al. (1988) indicate that group effects result in the lateral capacity of a pile group being less than the sum of the lateral capacities of the individual piles comprising the group. For in-line micropiles, group effects are negligible for micropile spacing between 6 and 7 diameters in the soil movement direction, and for micropiles arranged in a row (i.e., perpendicular to the direction of loading), group effects are negligible for micropile spacing of greater than just 3 diameters. For

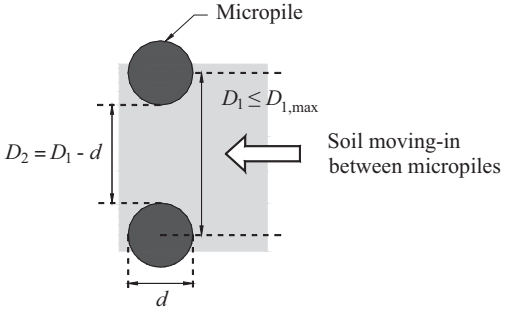

Fig. 7. Plastically deformation soil between two adjacent micropiles.

micropiles in a group in slope stabilization, the simplest approach is to use the suggestion of Sun et al. (2010) that micropile spacing at slip surface, $\overline{D_1}$ should be above 7 diameters in line to decrease the group reduction effects.

While it is recognized that micropiles for slope stabilization will typically include some vertical micropiles and battered micropiles connected at the ground surface via a concrete beam, the combined capacity of micropile group including vertical elements, battered upslope elements, and battered downslope elements, F_A, can be determined as

$$F_A = \sum F = F_1 + F_2 + F_3 \tag{25}$$

where F_1 is the shear capacity of battered upslope micropiles, F_2 is the shear capacity of vertical micropiles, and F_3 is the shear capacity of battered downslope micropiles.

4.5. Calculating the spacing required in row

It is clear that, in order to be effective, the following factors should be taken into account to determine the required micropile spacing in row: (1) the magnitude of resisting force provided by the micropile group must be at least equal to F_R; and (2) the distance between individual micropiles along the cap beam must be large enough to permit ease of construction of the micropile. The required micropile spacing in row, $D_{1,max}$ may be calculated as

$$D_{1,max} = \frac{F_A}{F_R} \tag{26}$$

If the soil above the slip surface is very weak or micropiles are spaced too far apart, there exists a potential for soil material to move in-between adjacent micropiles (Fig. 7). Ito and Matsui (1975) developed a theory to evaluate plastic flow between piles. Accordingly, the lateral force acting on the micropile, q is defined as

$$q = cD_1\left(\frac{D_1}{D_2}\right)^{(N_\varphi{}^{1/2}\tan\varphi + N_\varphi - 1)} \left[\frac{1}{N_\varphi \tan\varphi}\left\{\exp\left(\frac{D_1 - D_2}{D_2} N_\varphi \tan\varphi \tan\left(\frac{\pi}{8} + \frac{\varphi}{4}\right)\right) - 2N_\varphi{}^{1/2}\tan\varphi - 1\right\} + 2\tan\varphi + 2N_\varphi{}^{1/2} + \frac{N_\varphi{}^{-1/2}}{N_\varphi{}^{-1/2}\tan\varphi + N_\varphi - 1}\right] - c\left\{D_1 2\tan\varphi + 2N_\varphi{}^{1/2} + \frac{N_\varphi{}^{-1/2}}{N_\varphi{}^{1/2}\tan\varphi + N_\varphi - 1 - 2D_2 N_\varphi{}^{-1/2}}\right\}$$

$$+\frac{\gamma' z}{N_\varphi}\left\{D_1\left(\frac{D_1}{D_2}\right)^{(N_\varphi{}^{1/2}\tan\varphi+N_\varphi-1)}\exp\left(\frac{D_1-D_2}{D_2}N_\varphi\tan\varphi\tan\right)\left(\frac{\pi}{8}+\frac{\varphi}{4}\right)-D_2\right\} \quad (27)$$

where $N_\phi = \tan^2[(\pi/4)+(\phi/2)]$, D_1 is the center-to-center spacings, D_2 is the opening between micropiles, c is the cohesion of the soil, φ is the angle of internal friction of soil, γ' is effective unit weight of soil and z is an arbitrary depth from ground surface.

The ultimate horizontal force acting on the micropile due to soil movement between adjacent micropiles. F_q is the value for q intergrated over the length of the micropile from the slip surface to the cap beam.

For micropiles groups used for weak soil slope stabilization, the calculated F_q should be compared to the resistance provided by micropile group, F_A to evaluate the spacing between micropiles as shown below:

(1) For $F_q \geq F_A/2$, the plastic flow conditions do not govern, $D_1 = D_{1,\,max}$.
(2) For $F_q < F_A/2$, the plastic flow conditions govern, $D_1 < D_{1,\,max}$.

4.6. Structural design of concrete cap beam

The concrete cap beam spans and anchors the micropile array at the ground surface, which constrains the displacement of micropiles and improves the shear capacity to some extent. The structural design of the concrete cap beam follows typical methods for reinforced concrete in China (China National Standards GB50010-2002, 2002). The common concrete cap beam used in China is an embedded single strip foundation or the framework foundation. A single strip foundation is typically 2 m wide and 1 m deep, and in general, the cap beam should have sufficient height and width to allow for at least two to three micropile diameters embedment into the cap beam to promote fixity of the micropiles.

5. Example of application: K31 landslide, Qinghai, China

To study the effect of micropiles against landslide, an existing embankment landslide in Zhaba-Hacheng roadway in Qinghai was adopted as an example. The embankment was constructed nearly 30-years-ago, and had an approximate height of 30 m with an inclination of 35° (Fig. 8). An embankment landslide took place after a storm rainfall. As can be observed in Fig. 9, a gentle circular arc can appropriately represent the slip surface geometry. The appearance of the displaced mass clearly indicates that the failure was rather in the form of material flow.

5.1. Site conditions

There are two mainly geomaterial units in the embankment slope, which are the upper silty clay and the lower siltstone. The silty clay is about 5–10 m thick and the siltstone is weak weathered. Fig. 9 illustrates the groundwater flow path in the slope. The shear strength parameters adopted for the analyses are summarized in Table 1, which were obtained from limited laboratory tests following the China National Standards GB/T50123-1999 (1999).

Fig. 8. Image of the landslide.

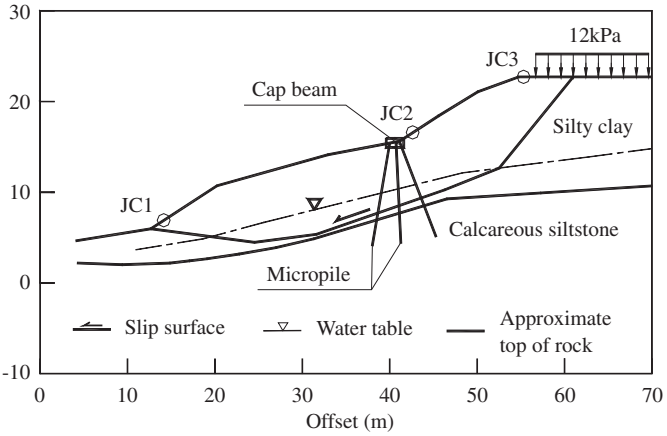

Fig. 9. Cross section of controlling project.

Table 1
Main physical and mechanical parameters of different layers in slope (CU).

Layer	γ (kN/m^3)	c (kPa)	φ (deg)
Silty clay	21.2	25	18
Calcareous siltstone	23	480	23

5.2. Scheme of stabilization

Slope movements resulted in pavement settlement and cracking, which caused the roadway to remain out of service for a long time. Two alternatives were considered for stabilization. One alternative consisted of regrading the slope and constructing anti-sliding piles and the other one was the use of micropiles. The anti-sliding piles were rejected for implementation because they were not cost effective. Micropiles were selected for implementation since they were less expensive than anti-sliding piles (savings

RMB780, 000) and could be constructed in highly variable ground and under restricted access conditions. Other advantages included the ability to maintain traffic during construction and minimal environmental impact.

5.3. Design of micropiles

The micropile cross section is selected as Type A in Fig. 6. The diameter of micropiles was 230 mm each. Each micropile was assumed to be reinforced with API-80 casing. The yield stress of the reinforcement was taken as 552 MPa. The ultimate bending moment, M_{ult} is evaluated by the method in Section 2, and the results are shown as follows:

(1) For $0^{\circ} \le \psi \le 10^{\circ}$, $N=0$, $M_{ult}=161.3kN\ m$;
(2) For $\psi \ge 30^{\circ}$, $N=475$kN, $M_{ult}=147.7kN\ m$.

A factor of safety of 1.3 was selected as the minimum adequate value following the Chinese standard GB 50330-2002, which is determined depending on the security level of the roadway. Micropiles were located at approximately a midslope location, accordingly, the additional force required from the micropile F_R is 650 kN/m. Local slope stability analyses were performed to confirm that slip surfaces upslope and downslope from the micropile location having an acceptable factor of safety. The results indicated that the miminum factor of safety for upslope slip surface was 1.30 and the minimum factor of safety for downslope slip surface was 1.35. Since these values are greater than 1.30, there was no need to take additional measures to increase the local slope stability.

Three rows of micropiles comprised the group, as can be seen in Fig. 9, the leading row of micropiles were battered 10°, the middle row was almost vertical, and the rear row of micropiles were battered 21°. The micropile length ranged between 15 and 18 m, with the spacings 1.5 m at in-row direction. The shear capacity of micropiles F_1–F_3 was 420 kN, 329 kN and 329 kN, respectively.

The main parameters adopted for p–y analyses are summarized in Table 2. The silty clay 1 and 2 represent the material above and below the water level, respectively. The effective unit weight (γ'), the undrained strength (c_u) and strain corresponding to one-half of the maximum principal stress difference (ε_{50}) were also obtained from laboratory tests.

The shear capacity of micropiles, F_A was calculated as 1078kN by Eq. (25). And the calculated micropile spacing required in row, $D_{1,\ max}$ is 1.65 m. The actual micropile spacing, $D_1=1.5$ m was adopted considering the site conditions. Besides, the plastic flow analysis was accomplished to check the potential soil flow between micropiles, and the results show the F_q was calculated to be 753 kN, which is above the half of F_A, so plastic flow will not take place under these circumstances.

The embedded steel-reinforced concrete cap beam was designed in a single strip, typically 1.5 m wide and 0.75 m deep. The length of embedment was 0.5 m for the micropiles into the cap beam.

Table 2
Parameters of layers in slope (UU).

Soil type	C_u (kN/m^3)	γ' (kN/m^3)	ε_{50}
Silty clay 1	120	21.2	0.0050
Silty clay 2	168	11.4	0.0040
Calcareous siltstone	480	13.2	0.0025

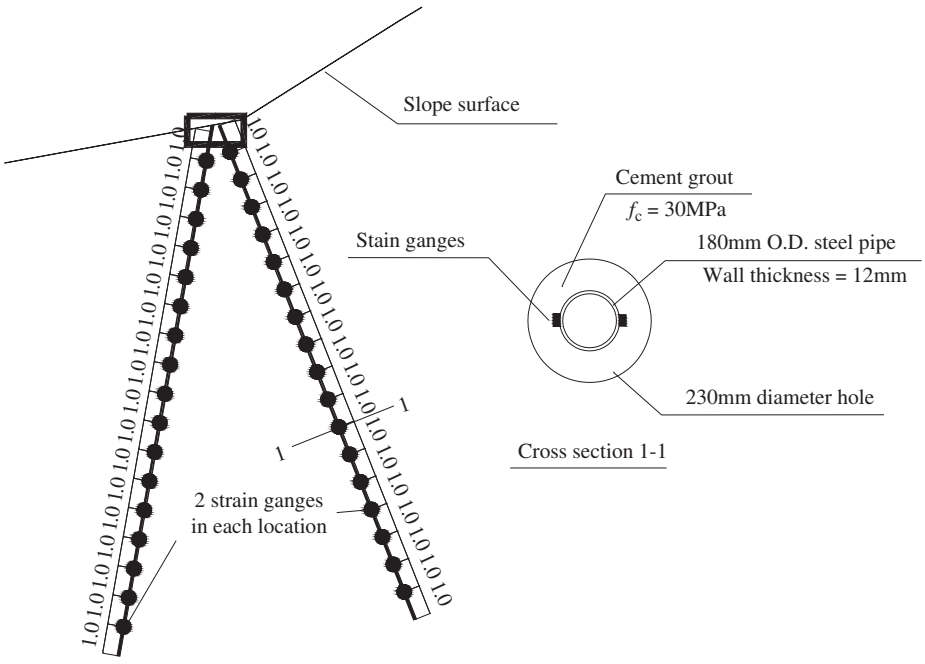

Fig. 10. Strain gauge locations on micropiles (Unit: m). (*Note*: the middle micropile is absent from the figure).

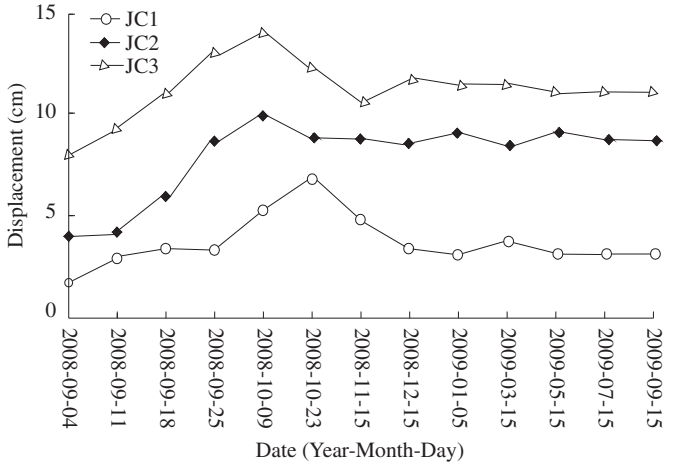

Fig. 11. Horizontal displacements of JC1–JC3.

6. Monitoring data

The k31 landslide was the first project in Qinghai in which micropiles were used to create a permanent landslide stabilization system. A comprehensive instrumentation and monitoring program was developed to assess the filed performance of the micropiles. Instrumentation consisted of 3 horizontal displacement monitoring points JC1–JC3 (seeing Fig. 9) and strain gauges attached micropile steel casings (seeing Fig. 10). Information collected included slope movement and load transfer of the micropiles.

Measured displacements of JC1–JC3 were shown in Fig. 11. The displacements were increasing at the beginning construction, and then decrease slightly over the time. The maximum value of horizontal displacement was about 15 cm. Two months after the construction (December 15 in 2008), the measured displacments ceased and remained constant. These results indicate that the micropiles were effective in reducing slope movements.

Measured axial loads in the micropiles were less than those assumed in the design (Fig. 12). In addition, the upslope battered micropiles and the downslope battered piles were both in tension and the maximum value is in the vincinity of the slide plane. The strain ganges also indicated higher bending momenting developed in the micropiles in the vicinity of the slide surface (Fig. 13). Measured maximum bending moments ranged from approximately 10 percent of the ultimate bending moment capacity of the micropiles. It should be pointed out that the measured maximum bending moment was far less than the ultimate bending moment capacity. There are two main factors resulting in the large gap: (1) The shear strength parameters of the embankment materials as determined from the testing program are based on the assumption that a standard compaction procedure had been implemented during construction of the embankment. The actual construction quality of the nearly 30-years-old embankment, however, is virtually unknown. (2) It is not easy to explain the field test result due to some uncertain factors, including difficulties maintaining and monitoring instrumentation, long testing periods, and change of testing conditions. In general, instrumentation data indicated that the micropiles performance was acceptable.

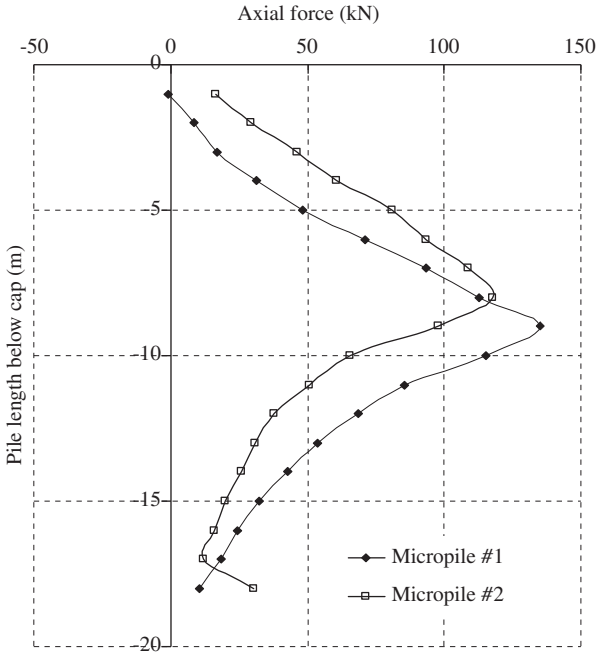

Fig. 12. Measured axial force of Micropile #1 and #2.

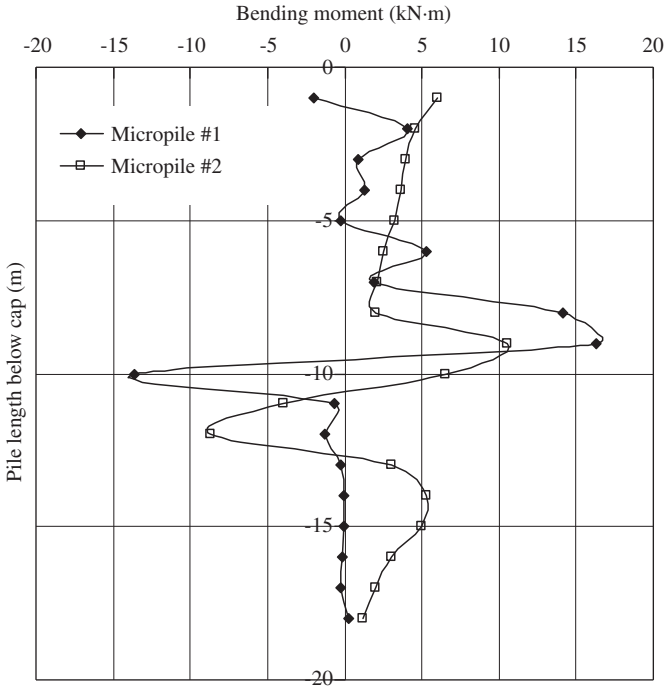

Fig. 13. Measured bending moment of Micropile #1 and #2.

7. Conclusions

An approach has been described for the design of micropiles to stabilize earth slopes.

- An analytic model was set up to determine the ultimate resistance of micropiles based on the conventional beam-column equation and existing p–y curve method. The micropile is analyzed in two sections to compute the displacement, bending moment, and shear force at each

point, and the solution was adopted by consideration of the compatibility of the pile head slope at the slip surface.

- A step-by-step procedure has been proposed for the design of micropiles in earth soil slope stabilization, including guidelines about choosing a location for micropiles within the existing slope, selecting the micropile cross section, estimating the length of micropile, evaluating the shear capacity of the micropile groups, calculating the required micropile spacing and the design of the concrete cap beam. Once a desired safety factor and the location of the micropiles are decided upon, the length of the micropile, the shear capacity of the micropiles, and the required micropile spacing can be determined.
- An application of the design approach in a roadway embankment landslide in China was described. Monitoring data indicated that slope movement had effectively ceased as a result of the slope stabilization measure, and micropiles performance was acceptable.

Acknowledgments

This work is supported by the National Natural Science Fundation of China (Grant nos. 41002090 and 51034005) and the Fundamental Research Funds for the Central Universities (Grant no. 2011QZ05). We would like to express our gratitude to the editors and reviewers for their constructive and helpful review comments.

References

Brown, D.A., Morrison, C., Reese, L.C., 1988. Lateral load behavior of pile group in sand. Journal of Geotechnical Engineering 114 (11), 1261–1276.

Bruce, D.A., Juran, I., 1997. Drilled and Grouted Micropiles: State-of-Practice Review. US Federal Highway Administration. Publication FHWA-RD-96-017, Washington, DC.

Cai, F., Ugai, K., 2000. Numerical analysis of the stability of a slope reinforced with piles. Soils and Foundations 40 (1), 73–84.

Cantoni, R., Collotta, T., Ghionna, V., 1989. A design method for reticulated micropiles structure in sliding slopes. Ground Engineering 22 (4), 41–47.

China National Standards GB/T50123-1999, 1999. Standard for soil test method, the standardization administration of China, the Ministry of Construction of China, and the Ministry of Water Resources of China. China Planning Press, Beijing (in Chinese).

China National Standards GB50010-2002, 2002. Code for design of concrete structures, Ministry of Construction of China. China Architecture & Building Press, Beijing (in Chinese).

Hognestad, E., 1951. A study of combined bending and axial load in reinforced concrete members. University of Illinois Engineering Experiment Station.

Holloway, D.M., Moriwaki, Y., Stevens, J.B., 1981. Response of a pile group to combined axial and lateral loading. In: Proceedings of the 10th International Conference on Soil Mechanics and Foundation Engineering. Stockholm.

Ito, T., Matsui, T., 1975. Methods to estimate lateral force acting on stabilizing piles. Soils and Foundations 15 (4), 45–59.

Juran, I., Benslimane, A., Bruce, D.A., 1996. Slope stabilization by micropile reinforcement. Landslides 5, 1718–1726.

Lizzi, F., 1978. Reticulated Root Piles to correct landslides, ASCE Convention, Chicago, Preprint 3370.

Lizzi, F., 1982. The pali radice (root piles), Symposium on Soil and Rock Improvement Techniques including Geotextiles, Reinforced Earth and Modern Piling Methods, Bangkok, Paper D-3.

Loehr, J.E., Bowders, J.J., Owen, J.W., 2000. Slope stabilization with recycled plastic pins. Journal of Transportation Research Record 1714, 1–8.

Matlock, H., 1970. Correlations for design of laterally loaded piles in soft clay. In: Proceedings of the Annual Offshore Technology Conference. Houston, Texas.

Palmerton, J.B., 1984. Stability of moving land masses by cast-in-place piles, Federal Highway Administration, Washington, DC, Final Report, Miscellaneous Paper GL-84-4.

Pearlman, S.L., Wolosick, J.R., 1992. Pin piles for bridge foundations. In: Proceedings of the 9th Annual International Bridge Conference. Pittsburgh, Pennsylvania.

Pearlman, S.L., Campbell, B.D., Withiam, J.L., 1992. Slope stabilization using in-situ earth reinforcement. In: Proceedings of a Special Conference on Stability and Performance of Slopes and Embankment, vol. 2. Berkeley, CA.

Pinyol, N.M., Alonso, E.E., 2012. Design of micropiles for tunnel face reinforcement: undrained upper bound solution. Journal of Geotechnical and Geoenvironmental Engineering 138, 89–99.

Plumelle, C., 1984. Improvement of the bearing capacity of soil by inserts of group and reticulated micro piles. International Symposium on in-situ reinforcement of soils and rocks., ENPC Press, Paris, pp. 83–89.

Poulos, H.G., 1995. Design of reinforcing piles to increase slope stability. Canadian Geotechnical Journal 32, 808–818.

Poulos, H.G., Davis, E.H., 1980. Pile Foundation Analysis and Design. John Wiley & Sons, New York.

Reese, L.C., Welch, R.C., 1975. Lateral loading of deep foundations in stiff clay. Journal of the Geotechnical Engineering Division 101 (7), 633–649.

Reese, L.C., Wang, S.T., Isenhower, W.M., 1992. Use of drilled shafts in stabilizing a slope. Stability and Performance of Slopes and Embankments 2 (31), 1318–1332.

Rusch, H., 1960. Researches toward a general flexural theory for structural concrete. Journal Proceedings 57 (7), 1–28.

Sun, S.W., Zhu, B.Z., Ma, H.M., 2009. Model tests on anti-sliding mechanism of micropile groups and anti-sliding piles. Chinese Journal of Geotechnical Engineering 31 (10), 1564–1570 (in Chinese).

Sun, S.W., Zhu, B.Z., Zheng, J., 2010. Design method of micropile group for soil slope stabilization based ultimate resistance of micropile. Chinese Journal of Geotechnical Engineering 32 (11), 1671–1677 (in Chinese).

Tsukada, Y., Miura, K., Tsubokawa, Y., Otani, Y., You, G.L., 2006. Mechanism of bearing capacity of spread footings reinforced with micropiles. Soils and Foundations 46 (3), 367–376.